Fidelity and superconductivity in two-dimensional *t-J* models

Marcos Rigol
Department of Physics, Georgetown University, Washington, DC 20057, USA

B. Sriram Shastry
Department of Physics, University of California, Santa Cruz, California 95064, USA

Stephan Haas
Department of Physics and Astronomy, University of Southern California, Los Angeles, California 90089, USA

(Received 29 June 2009; revised manuscript received 25 August 2009; published 29 September 2009)

We compute the ground-state fidelity and various correlations to gauge the competition between different orders in two-dimensional *t-J*-type models. Using exact numerical diagonalization techniques, these quantities are examined for (i) the plain *t-J* and *t-t′-J* models, (ii) for the *t-J* model perturbed by infinite-range *d*-wave or extended-*s*-wave superconductivity inducing terms, and (iii) the *t-J* model, plain and with a *d*-wave perturbation, in the presence of nonmagnetic quenched disorder. Various properties at low hole doping are contrasted with those at low electron filling. In the clean case, our results are consistent with previous work that concluded that the plain *t-J* model supports *d*-wave superconductivity. As a consequence of the strong correlations present in the low hole doping regime, we find that the magnitude of the *d*-wave condensate occupation is small even in the presence of large *d*-wave superconductivity inducing terms. In the dirty case, we show the robustness of the ground state in the strongly correlated regime against disorder.

DOI: 10.1103/PhysRevB.80.094529 PACS number(s): 75.10.Jm, 05.50.+q, 05.70.−a

I. INTRODUCTION

Understanding the mechanism of high-temperature superconductivity has remained a subject of much interest since its experimental discovery in the cuprates in 1986.[1] More recently, this subject has received renewed attention following the emergence of the first iron based (pnictide) high-temperature superconductor.[2] It is generally believed that high-temperature superconductivity has its roots in the interplay of strong correlations and reduced dimensionality.[3–5] However, a full theoretical understanding of this phenomenon has proven challenging, and consensus regarding its microscopic origin has not yet been reached.[6–9]

A further complication arises from experimental findings that the doped cuprates are highly inhomogeneous.[10] This feature has been the subject of numerous recent experimental studies using local probes such as scanning tunneling spectroscopy (STS).[11–16] Theoretical studies of correlations and disorder in superconducting lattice models have, in general, either focused on *d*-wave BCS phenomenology in the presence of impurities[17–19] or on microscopic disordered *t-J* and Hubbard type models, sometimes with the addition of short-ranged terms that favor superconductivity. One basic result of BCS phenomenology is that nonmagnetic impurities suppress superconductivity more strongly in nodal systems, i.e., *d*-wave superconductors, than in conventional *s*-wave superconductors.[17–20] This raises the question why superconductivity in the high-temperature cuprates appears to be rather resistant to impurity disorder, although they have a *d*-wave superconducting order parameter. A large part of the answer presumably involves the short coherence length, which is of the order of a few lattice constants in these systems, as opposed to the enormous values attained in conventional superconductors. Another problem within the standard BCS phenomenology appears to be that the only way correlations enter is through superconducting pairing channels, neglecting potentially important effects due to the presence of fluctuations toward other competing instabilities. The robustness of high-temperature superconductivity and its density of states against disorder has been recently studied in the framework of Hubbard and *t-J* models using Bogoliubov–de Gennes[21,22] and Gutzwiller mean-field theories,[21] and exact diagonalization.[23]

In a spirit similar to previous studies,[3,23] in this work we use numerical diagonalization of finite clusters to examine the effects of doping a strongly correlated Mott insulator within the *t-J* model. The *t-J* model can be justified microscopically either by a large U/t expansion of the one-band Hubbard model[3,5] or by a reduction of the three-band copper oxide model to an effective single-band model.[24,25] The latter approach provides greater freedom for the allowed parameter ratio of $J/|t|$. Following Ref. 23, we also consider the *t-J* model with the addition of an infinite-range superconducting term. This term is tunable, and structured to induce either *d*-wave or extended-*s*-wave superconductivity. Furthermore, we analyze the effects of quenched disorder in the ground state of these systems.

In this work, we focus on three key observables that provide unique insights into the properties of the *t-J* model. The first of these observables is the ground-state fidelity metric g, defined below in Eq. (10). This quantity is related to the rate of change of the overlap between the ground states of two Hamiltonians induced by a small change of a control parameter. The ground-state fidelity, originally studied in the context of quantum information theory, has been shown to be a sensitive indicator of changes in the ground state of many-body systems, as they occur in quantum phase transitions.[26–34] The other two observables of interest we will study are the *d*-wave and extended-*s*-wave superconductivity

condensate occupations. They will be defined carefully in the next section.

A few words motivating this project and the tools used are appropriate at this point. By changing control parameters in a quantum many-body system, one may encounter first-order or continuous quantum phase transition. In finite systems, first-order transitions are easy to monitor, using the ground-state energy and density matrices. We have studied pair-pair (with *d*-wave and extended-*s*-wave symmetries) and density-density/spin-spin correlations. The former indicate superconducting instabilities and the latter indicate charge or spin orderings. Continuous transitions are more subtle. Due to the Wigner–von Neumann noncrossing rule, different states of the same symmetry approach each other near a transition but do not cross; thereby leading to energy gaps. These energy gaps ultimately close for very large systems at quantum phase transitions. In recent work, the fidelity [Eq. (7)], and especially the associated fidelity metric [Eq. (10)], have been shown to be sensitive indicators of continuous transitions,[26–33] and we will see below that these also track level crossings quite well, as in general g exhibits a jump in those cases.

The paper is organized as follows. First, the *t*-*J* model and the observables of interest are described in Sec. II. Sec. III describes our study of the plain *t*-*J* and *t*-*t*′-*J* models when tuning the ratio J/t. In Sec. IV, we examine the *t*-*J* model with the addition of *d*-wave and extended-*s*-wave superconductivity inducing terms. The effects of quenched disorder in the fidelity and superconductivity order parameters are analyzed in Sec. V. In Sec. VI, we conclude with a summary of our findings.

II. PRELIMINARIES

A. Model Hamiltonians

The Hamiltonian for the plain *t*-*J* model can be written as

$$\hat{\mathcal{H}}_{tJ} = -t \sum_{\langle i,j\rangle,s} \hat{P}(\hat{c}_{is}^{\dagger}\hat{c}_{js} + \text{H.c.})\hat{P} + J\sum_{\langle i,j\rangle} \hat{P}\left(\hat{\mathbf{S}}_i \cdot \hat{\mathbf{S}}_j - \frac{1}{4}\hat{n}_i\hat{n}_j\right)\hat{P}, \tag{1}$$

where $\hat{c}_{is}^{\dagger}$ and $\hat{c}_{is}$ are the creation and annihilation operators for an electron with spin $s=\uparrow,\downarrow$ on a site i, $\hat{n}_i=\Sigma_s \hat{c}_{is}^{\dagger}\hat{c}_{is}$ is the density operator, $\hat{P}$ is a projection operator to ensure that there are no doubly occupied sites, i.e., it is assumed that the local Coulomb repulsion is very large such that two electrons (with antiparallel spin) cannot be on the same lattice site, and

$$\hat{\mathbf{S}}_i = \frac{1}{2}\sum_{ss'} \hat{c}_{is}^{\dagger}\boldsymbol{\sigma}_{ss'}\hat{c}_{is'} \tag{2}$$

is the local spin operator ($\boldsymbol{\sigma}$ are the spin-1/2 Pauli matrices). The sums $\langle i,j\rangle$ in Eq. (1) run over nearest-neighbor sites.

It has been discussed is several works that longer-range hoppings are needed to reproduce the Fermi surface and electron-hole asymmetries for different cuprate superconductors.[35–41] Here we will briefly discuss the effect of the next-nearest-neighbor hopping

$$\hat{\mathcal{H}}_{t'} = -t' \sum_{\langle\langle i,j\rangle\rangle,s} \hat{P}(\hat{c}_{is}^{\dagger}\hat{c}_{js} + \text{H.c.})\hat{P}, \tag{3}$$

where now the sum $\langle\langle i,j\rangle\rangle$ runs over next-nearest-neighbor sites.

Within a number of mean-field theories,[42–44] the phase diagram of the doped *t*-*J* model exhibits *d*-wave superconductivity. However, it is not clear how quantum fluctuations, which are expected to be significant in two dimensions, would affect such a state. As suggested by numerical diagonalization[45–47] and quantum Monte Carlo studies,[48,49] competing states with other broken symmetries are expected to occur in the proximity of the superconducting phase. In particular, there has been a debate within the literature whether at low hole doping, phase separation in the two-dimensional case occurs already at infinitesimal $J/t>0$ or only beyond a finite threshold value,[48–52] preceded by *d*-wave superconductivity.[45–47] It thus appears that the exact phase diagram of the *t*-*J* model still remains to be settled. Here, we address some of these issues using the fidelity as an indicator. Meanwhile, in order to precipitate a superconducting ground state in the presence of strong correlations, we add attractive terms of the form

$$\hat{\mathcal{H}}_d = -\frac{\lambda_d}{L}\sum_{i,j=1}^{L} \hat{P}\hat{\mathcal{D}}_i^{\dagger}\hat{\mathcal{D}}_j\hat{P}, \tag{4}$$

which favors a *d*-wave superconducting pairing, and

$$\hat{\mathcal{H}}_s = -\frac{\lambda_s}{L}\sum_{i,j=1}^{L} \hat{P}\hat{\mathcal{S}}_i^{\dagger}\hat{\mathcal{S}}_j\hat{P}, \tag{5}$$

which favors an extended-*s*-wave superconducting pairing.

In Eqs. (4) and (5), $\hat{\mathcal{D}}_i=(\hat{\Delta}_{i,i+\hat{x}}-\hat{\Delta}_{i,i+\hat{y}})$, $\hat{\mathcal{S}}_i=(\hat{\Delta}_{i,i+\hat{x}}+\hat{\Delta}_{i,i+\hat{y}})$ and $\hat{\Delta}_{ij}=\hat{c}_{i\uparrow}\hat{c}_{j\downarrow}+\hat{c}_{j\uparrow}\hat{c}_{i\downarrow}$. λ_d and λ_s denote the strengths of the *d*-wave and extended-*s*-wave superconductivity inducing terms, respectively, and L is the number of lattice sites. Equations (4) and (5) have infinite-range terms of the type Bardeen, Cooper, and Schrieffer considered in their reduced Hamiltonian,[53] while building in the *d*-wave and extended-*s*-wave symmetries in the superconductivity order parameter. Within mean-field theory, Eq. (1) with the addition of Eq. (4) leads to the same *d*-wave ground state as found from the *t*-*J* model.[42,43]

Finally, we also consider the effects of quenched random disorder of the form

$$\hat{\mathcal{H}}_{random} = \sum_i \varepsilon_i\hat{n}_i, \tag{6}$$

where the ε_i's are taken randomly from a uniform distribution between $[-\Gamma,\Gamma]$. The full Hamiltonians given by Eqs. (1)–(6) thus describe inhomogeneous strongly correlated superconductors. In this study, we use numerical diagonalization of clusters with 18 and 20 sites and periodic boundary conditions. The cluster geometries can be found in Ref. 3. The dimension of the largest Hilbert space diagonalized is of the order of 10^8.

B. Observables

The first observable of interest is related to the fidelity F, which is defined as follows. Assume a general Hamiltonian of the form

$$\hat{\mathcal{H}}(\lambda) = \hat{\mathcal{H}}_0 + \lambda \hat{\mathcal{H}}_1,$$

where $\hat{\mathcal{H}}_1$ is taken to be the driving term. In the next sections, we will consider $\hat{\mathcal{H}}_1$ to be either the Heisenberg interaction term in Eq. (1), the superconducting terms given by Eqs. (4) and (5), or the disorder term in Eq. (6). Let $|\Psi_0(\lambda)\rangle$ be the (normalized) ground state of $\hat{\mathcal{H}}(\lambda)$ and $|\Psi_0(\lambda+\delta\lambda)\rangle$ be the (normalized) ground state of $\hat{\mathcal{H}}(\lambda+\delta\lambda)$. The fidelity is then defined as the overlap between $|\Psi_0(\lambda)\rangle$ and $|\Psi_0(\lambda+\delta\lambda)\rangle$, i.e.,

$$F(\lambda, \delta\lambda) = |\langle \Psi_0(\lambda) | \Psi_0(\lambda + \delta\lambda)\rangle|. \tag{7}$$

If the ground state is nondegenerate, and if $\delta\lambda$ is sufficiently small, one can compute $|\Psi_0(\lambda+\delta\lambda)\rangle$ up to second order in perturbation theory. The only two terms of the (normalized) second order expansion that have a nonvanishing overlap (n.o.) with $|\Psi_0(\lambda)\rangle$ are

$$|\Psi_0(\lambda+\delta\lambda)\rangle_{\text{n.o.}} = |\Psi_0(\lambda)\rangle \times \left(1 - \frac{\delta\lambda^2}{2} \sum_{\alpha\neq 0} \frac{|\langle \Psi_\alpha(\lambda)|\hat{\mathcal{H}}_1|\Psi_0(\lambda)\rangle|^2}{[E_0(\lambda) - E_\alpha(\lambda)]^2}\right), \tag{8}$$

where $|\Psi_\alpha(\lambda)\rangle$ are the eigenstates of the Hamiltonian with eigenenergies $E_\alpha(\lambda)$, i.e., $\hat{\mathcal{H}}(\lambda)|\Psi_\alpha(\lambda)\rangle = E_\alpha(\lambda)|\Psi_\alpha(\lambda)\rangle$.

This means that up to the lowest order in $\delta\lambda$, one can write the fidelity in the form

$$F(\lambda, \delta\lambda) = 1 - \frac{\delta\lambda^2}{2} \sum_{\alpha\neq 0} \frac{|\langle \Psi_\alpha(\lambda)|\hat{\mathcal{H}}_1|\Psi_0(\lambda)\rangle|^2}{[E_0(\lambda) - E_\alpha(\lambda)]^2}. \tag{9}$$

Since the sum on the rhs is in most cases an extensive quantity (see, e.g., Refs. 28, 31, and 32; for counterexamples see, e.g., Ref. 34), one can define the fidelity metric as

$$g(\lambda, \delta\lambda) \equiv \frac{2}{L} \frac{1 - F(\lambda, \delta\lambda)}{\delta\lambda^2}$$

$$\lim_{\delta\lambda\to 0} g(\lambda, \delta\lambda) = \frac{1}{L} \sum_{\alpha\neq 0} \frac{|\langle \Psi_\alpha(\lambda)|\hat{\mathcal{H}}_1|\Psi_0(\lambda)\rangle|^2}{[E_0(\lambda) - E_\alpha(\lambda)]^2}. \tag{10}$$

In the following, we refer to $\lim_{\delta\lambda\to 0} g(\lambda, \delta\lambda)$ as $g(\lambda)$ or simply as g. From its definition, the fidelity metric g is dimensionless, positive and (in most cases) intensive, i.e., of $O(1)$. This is one of the main quantities that we will examine in the following sections. $F(\lambda, \delta\lambda)$ will be computed using Lanczos diagonalization, choosing a value of $\delta\lambda$ that is sufficiently small so that it does not affect the result of the ratio in Eq. (10), i.e., giving effectively the value in the $\lim_{\delta\lambda\to 0} g(\lambda, \delta\lambda)$. The above is of course true provided one does not encounter a level crossing. At a crossing, we compute g on either side of its jump by the above limiting process.

The other two quantities of interest are the d-wave and extended-s-wave superconductivity condensate occupations. Given the d-wave pair density matrix

$$P^d_{ij} = \langle \Psi_0 | \hat{P} \hat{\mathcal{D}}^\dagger_i \hat{\mathcal{D}}_j \hat{P} | \Psi_0 \rangle, \tag{11}$$

and the extended-s-wave pair density matrix

$$P^s_{ij} = \langle \Psi_0 | \hat{P} \hat{\mathcal{S}}^\dagger_i \hat{\mathcal{S}}_j \hat{P} | \Psi_0 \rangle, \tag{12}$$

the d-wave (Λ^d_1) and extended-s-wave (Λ^s_1) condensate occupations are defined as the largest eigenvalues of P^d_{ij} and P^s_{ij}.[54] The corresponding eigenvectors of the density matrices are known as the "natural orbitals," and those with the largest eigenvalues are referred to as the "lowest natural orbitals.[55]" If a condensate of pairs with a particular symmetry occurs in the system, the corresponding condensate occupation will scale linearly with the total number of fermions, as the system size L is increased while keeping the density constant.[54] This in turn is equivalent to stating that P^d_{ij} and P^s_{ij} exhibit off-diagonal long-range order.[56] Condensation also implies that all other eigenvalues are $\Lambda^{d,s}_\alpha \sim O(1)$.[57] An advantage of using these definitions is that they are valid independently of whether the system is translationally invariant or not, i.e., they work the same in clean systems and in the presence of disorder. In the particular case of translationally invariant systems, the eigenvalues P^d_{ij} and P^s_{ij} are occupations in momentum space.

Since we will be dealing here with systems with different densities and finite sizes, in many cases we find it useful to monitor the ratios $R^d = \Lambda^d_1/\Lambda^d_2$ and $R^s = \Lambda^s_1/\Lambda^s_2$ between the largest eigenvalues $(\Lambda^d_1, \Lambda^s_1)$ and the second largest eigenvalues $(\Lambda^d_2, \Lambda^s_2)$ of the density matrices. These ratios were first introduced in our earlier work,[23] and here we briefly reiterate the motivation behind this construction. If condensation occurs, i.e., symmetry is broken in the thermodynamic limit, these are equivalent to studying Λ^d_1 and Λ^s_1 because the next eigenvalue is small, i.e., $\Lambda^{d,s}_2 \sim O(1)$. However, computing R^d and R^s has the added benefit of eliminating uninteresting normalization effects related to the change in the particle density, etc. It also has some advantages when trying to understand the effects of changing a Hamiltonian parameter for a system with a fixed size, where we find cases with Λ_1 and R behaving differently.

III. PLAIN t-J MODEL

As a first step, in this section we study how the observables of interest behave within the plain t-J model. We begin with the effect of the antiferromagnetic Heisenberg coupling on the ground state of this system. Within many mean-field theories, finite values of J favor superconducting ground states close to half-filling.[42–44] The energy scale is set by the hopping parameter $t=1$. We further study the ground state of the t-J model for values of J between 0 and 1. While this rather large range is not achievable within the large U/t expansion of the one-band Hubbard model (where $J \sim t^2/U$), it should rather be regarded as a "Gedanken range," intended

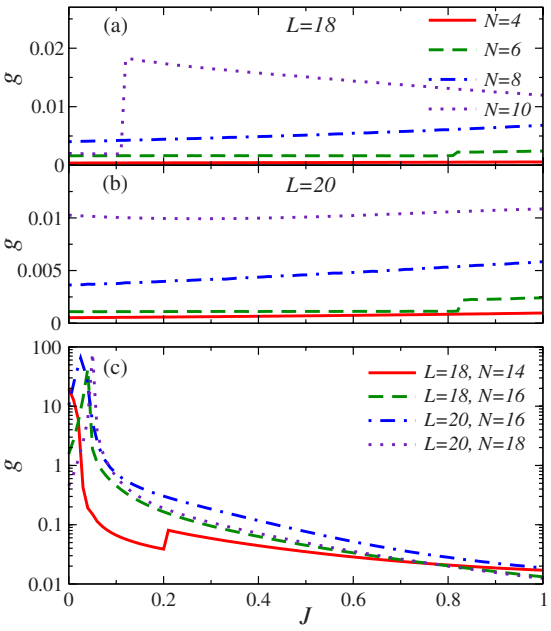

FIG. 1. (Color online) Fidelity metric of the t-J model as a function of the antiferromagnetic coupling J. (a) Cluster with 18 sites and fillings $N=4,6,8,10$. (b) Cluster with 20 sites and fillings $N=4,6,8,10$ [the same parameter sets as in (a)]. (c) Clusters with 18 and 20 sites and two and four holes. Notice that for all our results in this paper we consider $N=N_\uparrow+N_\downarrow$, where $N_\uparrow=\langle\hat{c}_\uparrow^\dagger\hat{c}_\uparrow\rangle$, $N_\downarrow=\langle\hat{c}_\downarrow^\dagger\hat{c}_\downarrow\rangle$, and $N_\uparrow=N_\downarrow$.

for the purpose of studying the possible phases that emerge, including the widely discussed possibility of phase separation.[47,50,51]

We begin by computing the fidelity metric in Eq. (10), considering the Heisenberg coupling in Eq. (1) to be the tuning parameter in the Hamiltonian, so that J plays the role of λ. For our computations, we find that taking $\delta J=10^{-5}$ is small enough to provide results for g which are independent of δJ.

In Fig. 1, we compare the dependence of the fidelity metric on J for low electron filling [Figs. 1(a) and 1(b)] and low hole filling [Fig. 1(c)]. The contrast between the two cases is very clear. For low electron filling the fidelity changes very little between $J=0$ and 1, but we do observe some level crossings, signaled by relatively small jumps in the fidelity metric. These have their origin in the peculiarities of particular cluster shapes, as exemplified by the fact that for the same particle number they are found in one of the clusters and not in the other (see, e.g., the case of ten particles), and therefore they are expected to disappear in the thermodynamic limit.

For low hole doping, on the other hand, see Fig. 1(c), the fidelity metric exhibits a large response for small $J\lesssim 0.05$, suggestive of a continuous phase transition in that regime. The cluster sizes accessible to numerical diagonalization are too small to identify a critical point, if any, but we find that a qualitatively similar behavior occurs for two and four holes in both clusters with 18 and 20 sites.

Next consider the occupation of the d-wave and extended-s-wave lowest natural orbitals as J is tuned in the system. Results for these quantities are shown in Fig. 2. As observed here, changes in the fidelity metric in Fig. 1 are

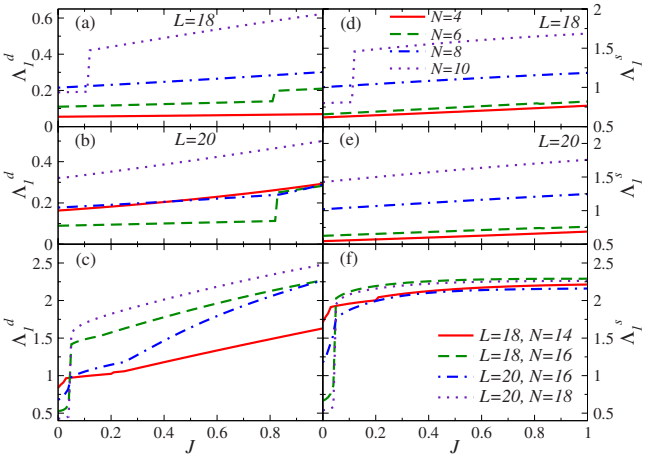

FIG. 2. (Color online) Occupation of the lowest natural orbital, of the d-wave (left panels) and extended-s-wave (right panels) density matrices, as a function of J. [(a) and (d)] Cluster with 18 sites and fillings $N=4,6,8,10$. [(b) and (e)] Cluster with 20 sites and fillings $N=4,6,8,10$. Notice that the parameter sets for (a)–(e) are all the same and given in (d). [(c) and (f)] Clusters with 18 and 20 sites and two and four holes. The parameter sets in (c) and (f) are also the same.

accompanied by changes in the lowest natural orbital occupations in Fig. 2. Interestingly, for each given cluster shape and filling fraction, the behavior of $\Lambda_1^d(J)$ and $\Lambda_1^s(J)$ is qualitatively similar. We do find, however, a marked difference between the results obtained for Λ_1^d and Λ_1^s between low electron filling, and low hole doping. For low electron filling [Figs. 2(a), 2(b), 2(d), and 2(e)], the lowest natural orbital occupation only changes appreciably when a level crossing is observed in the fidelity (Fig. 1). Also, in this case, we find $\Lambda_1^s>\Lambda_1^d$, suggesting dominant s-wave order parameter that is consistent with the results in Refs. 46 and 47. In contrast, for low hole doping [Figs. 2(c) and 2(f)] with two and four holes in both cluster geometries, the occupation of the lowest natural orbitals in all cases exhibit a large increase for small values of J ($J\lesssim 0.05$), where a sizable response was observed in g in Fig. 1.

It is interesting to observe that the occupation of the lowest natural orbitals of both d-wave and extended-s-wave symmetries in general increase as a result of increasing J. Since we cannot perform finite size scaling by studying larger systems, this does not throw light on the competition between these two orderings. In order to resolve this issue, we have also studied the ratio between the lowest two natural orbitals for both superconducting symmetries. The results are presented in Fig. 3. They show a quite different behavior from the one seen for the lowest natural orbitals in Fig. 2. We see from Figs. 3(a), 3(b), 3(d), and 3(e), that for low electron filling the ratio R between the two lowest natural orbitals in general remains almost unchanged when J takes values between 0 and 1, for both d-wave symmetry and extended-s-wave symmetry. For low hole doping, Figs. 3(c) and 3(f), the behavior is different. R^d increases for both two and four holes in 18 and 20 lattice sites, whereas R^s decreases for the same set of parameters. This is a strong indication that for larger systems sizes the model may select, if

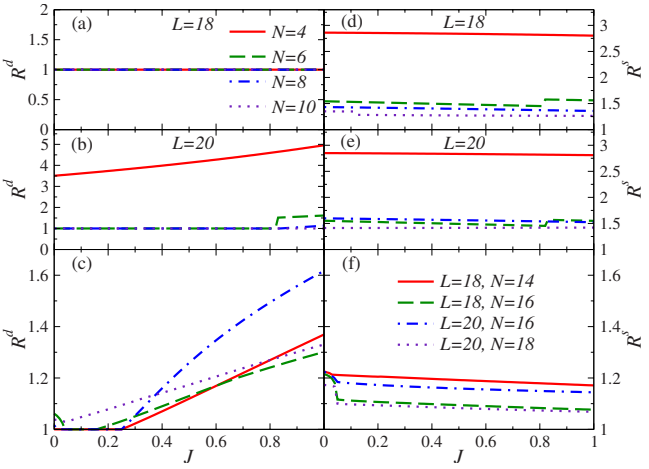

FIG. 3. (Color online) Ratio between the two lowest natural orbitals, of the *d*-wave (left panels) and extended-*s*-wave (right panels) density matrices, as a function of J. [(a) and (d)] Cluster with 18 sites and fillings $N=4,6,8,10$. [(b) and (e)] Cluster with 20 sites and fillings $N=4,6,8,10$. Notice that the parameter sets for (a)–(e) are all the same and given in (a). [(c) and (f)] Clusters with 18 and 20 sites and two and four holes. The parameter sets in (c) and (f) are also the same.

any, a *d*-wave superconducting ground state. To further explore this possibility, in the next section we perturb the *t*-*J* model Hamiltonian with *d*-wave and extended-*s*-wave superconductivity inducing terms and study its response.

We have also studied other correlation functions, such as the spin-spin and density-density correlations. The results for the ratio between the two lowest natural orbitals of those two matrices are presented in Fig. 4 for two and four holes in 18 and 20 sites. As expected, spin-spin correlations ($R^{ss-corr}$) exhibit a large enhancement corresponding to the onset of antiferromagnetic order. $R^{ss-corr}$ reduces dramatically as the hole doping increases, in contrast to the behavior of R^d in Fig. 3(c), which for large J increases as the doping increases (in the underdoped regime). Interestingly, stripes are expected to be one of the competing orders at low doping, and they should be reflected in the density-density structure factor (in $R^{dd-corr}$). In Fig. 4(b), one can see that $R^{dd-corr}$ actually decreases with increasing J, i.e., no signature of charge-density order can be seen in our clusters.

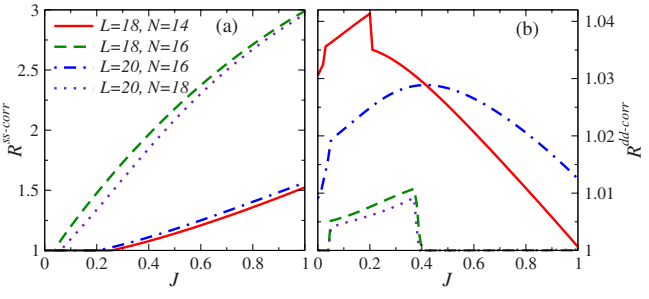

FIG. 4. (Color online) Ratio between the two lowest natural orbitals as a function of J in clusters with two and four holes with 18 and 20 lattice sites for (a) the spin-spin correlation matrix and (b) the density-density correlation matrix.

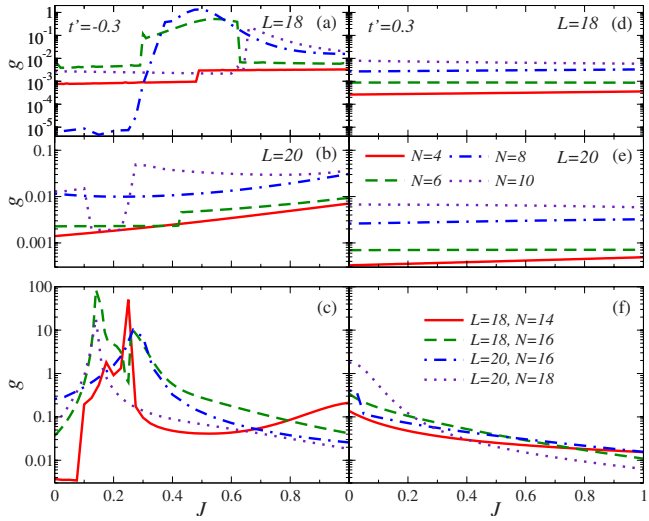

FIG. 5. (Color online) Fidelity metric of the *t*-*t*′-*J* model as a function of the antiferromagnetic coupling J for (a)–(c) $t'=-0.3$ and (d)–(f) $t'=0.3$. [(a) and (d)] Cluster with 18 sites and fillings $N=4,6,8,10$. [(b) and (e)] Cluster with 20 sites and fillings $N=4,6,8,10$ [the legends in (a), (b), and (d) are the same as in (e)]. [(c) and (f)] Clusters with 18 and 20 sites and two and four holes (the legends are the same in both figures).

Next-nearest-neighbor (t') term

As mentioned in Sec. II, several authors have discussed the importance of introducing long-range hopping in microscopic Hubbard and *t*-*J*-like models in order to capture many of the features observed in high-temperature superconductors.[35,36,38–41] Here, we briefly discuss how a finite next-nearest-neighbor hopping affects the results discussed above for the plain *t*-*J* model.

In Fig. 5, we show the fidelity metric for exactly the same clusters and fillings as in Fig. 1. The results in the presence of a finite and small t' are qualitatively similar to those of the plain *t*-*J* model [Fig. 1] in both the low-electron-filling and low-hole-doping regimes, and for negative (left column) and positive (right column) values of t'. It is worth noticing, however, that in the low doping regime the presence of a finite $t'<0$ [Fig. 5(c)] moves the maximum response of the fidelity metric toward larger values of J, while no such effect is seen for $t'>0$ [Fig. 5(f)]. The former displacement for $t'<0$ is more pronounced for four holes than for two holes in both clusters with 18 and 20 sites. This is consistent with previous works which have pointed out that in hole-doped systems t' competes with J as it suppresses both antiferromagnetic correlations[58–60] and the superconducting T_c,[60,61] and that the effect of t' becomes stronger with doping (in the low-hole-doping regime). A positive t', on the other hand, enhances antiferromagnetic correlations, which is consistent with the results in [Fig. 5(f)] where the maximum response of the fidelity is in all cases seen at $J=0$.

The results for the lowest natural orbitals and the ratio between the lowest the second lowest natural orbitals are also qualitatively similar to those of the plain *t*-*J* model, and will not be presented here. In the remaining of the paper, we will set $t'=0$ and study the effects of superconductivity enhancing terms and disorder in the *t*-*J* model.

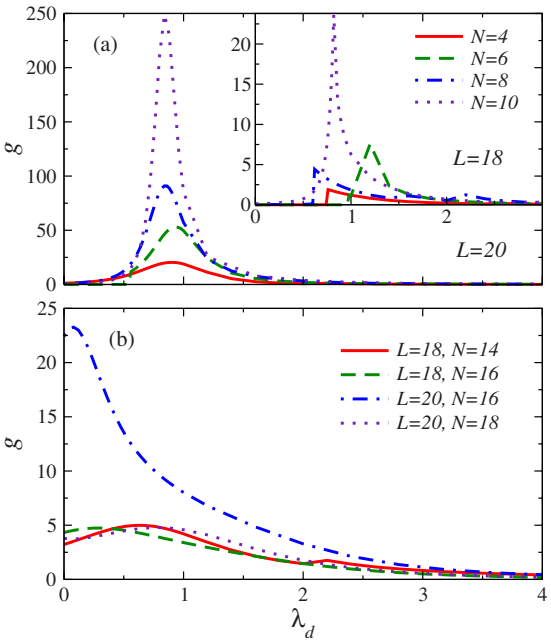

FIG. 6. (Color online) Fidelity metric of the t-J model ($J=0.3$) after the addition of a d-wave-superconductivity inducing term. (a) Cluster with 20 sites and fillings $N=4,6,8,10$. (b) Clusters with 18 and 20 sites and two and four holes. The inset in (a) depicts the results for the cluster with 18 sites and fillings $N=4,6,8,10$.

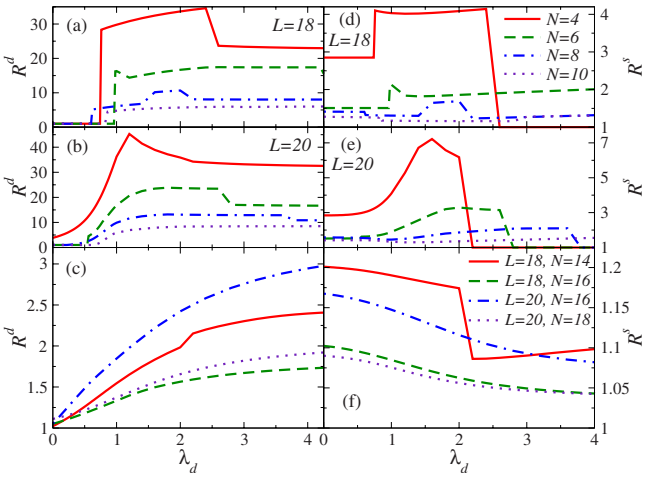

FIG. 7. (Color online) Ratio between the two lowest natural orbitals, of the d-wave (left panels) and extended-s-wave (right panels) density matrices, as a function of λ_d. [(a) and (d)] Cluster with 18 sites and fillings $N=4,6,8,10$. [(b) and (e)] Cluster with 20 sites and fillings $N=4,6,8,10$. Notice that the parameter sets for (a)–(e) are all the same and given in (d). [(c) and (f)] Clusters with 18 and 20 sites and two and four holes. The parameter sets in (c) and (f) are also the same.

IV. SUPERCONDUCTIVITY INDUCING TERMS

A. d-wave term

Let us first consider a total Hamiltonian that is the sum of Eq. (1) and the d-wave-superconductivity inducing term in Eq. (4), and study the ground state of this model as a function of increasing the parameter λ_d. In the following, we fix the Heisenberg coupling to be $J=0.3$, which is a value commonly used in the t-J model literature. From the analysis in the previous section, we know that, at least for the finite clusters considered here, no further qualitative changes occur in the observables of interest for larger values of J.

Recall from previous work,[23] that the added d-wave term Eq. (4), being of infinite range, must certainly precipitate superconductivity in the d-wave channel. This is because mean-field theory becomes exact in the thermodynamic limit for an infinite-range model of this type. (The same argument, of course, also works in the presence of an extended-s-wave term.) While this argument is true for very large systems, for finite systems one may need a finite $\lambda_d \sim O(1)$ to achieve superconductivity.[62] Therefore, we expect that in some cases the fidelity metric should show an enhancement as a function of λ_d at some characteristic value λ_d^*. A small value of λ_d^*, consistent with $\lambda_d^* \sim 0$, may be taken as an indicator of the incipient order of the $\lambda_d=0$ model (the plain t-J model).

In Fig. 6, we show the fidelity metric as a function of the driving parameter λ_d. In our calculations, we have taken $\delta\lambda_d=10^{-5}$, which is sufficiently small to ensure results consistent with the limit $\delta\lambda_d \to 0$.

Results for low electron fillings are shown in Fig. 6(a) and its inset. In all cases one can see that there is almost no response in g when λ_d is small and that a strong response occurs for $\lambda_d^* \sim 1$, indicative of a phase transition for a finite value of λ_d. These results are consistent with the behavior of the ratios R^d and R^s, which are depicted in Figs. 7(a), 7(b), 7(d), and 7(e). For most low fillings, both ratios change very little for small values of λ_d. Around $\lambda_d \sim 1$, they either jump abruptly (cluster with $L=18$) or increase rapidly (cluster with $L=20$). Notice that for large λ_d there is almost one order of magnitude difference between the ratios seen for the occupation of the d-wave related natural orbitals and the extended-s-wave related orbitals. This is expected since the driving term has d-wave symmetry and hence d-wave superconductivity should be stabilized for large values of λ_d.

The results for low hole doping (two and four holes) are in contrast with those of low electron filling. Figure 6(b) shows that in the former case g exhibits a large response for very small values of λ_d. The behavior of g in this case is consistent with a phase transition at $\lambda_d \sim 0$. The situation is similar to that of g in the one-dimensional Hubbard model as one tunes the onsite repulsion parameter U,[32] where the Mott phase transition occurs at $U=0$. In addition, as shown in Fig. 7(c) and 7(f), the response of g for small values of λ_d is accompanied by a continuous increase of R^d and a continuous decrease of R^s for small values of λ_d.

Comparing the results in this subsection with Sec. III, we find support for the view that in the thermodynamic limit, the plain t-J model is superconducting (with d-wave symmetry, for finite values of J), without the need of introducing λ_d. Finite values of λ_d certainly enhance the superconducting features of the t-J model in finite clusters but may not be needed for larger system sizes. Earlier evidence in this direction comes from high temperature expansion studies,[63] and exact diagonalization studies of the plain t-J model.[3,45–47]

We should stress that the magnitudes of the ratios R^d in Fig. 7(c), reveals a very important characteristic of the

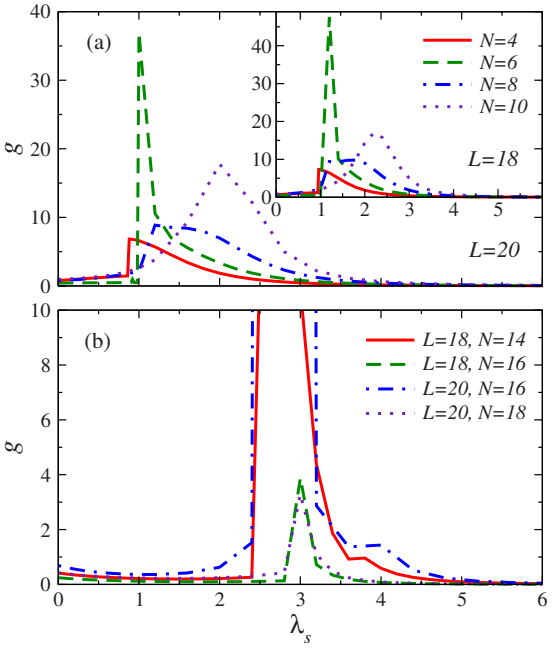

FIG. 8. (Color online) Fidelity metric of the t-J model ($J=0.3$) after the addition of an extended-s-wave-superconductivity inducing term. (a) Cluster with 20 sites and fillings $N=4,6,8,10$. (b) Clusters with 18 and 20 sites and two and four holes. The inset in (a) depicts the results for the cluster with 18 sites and fillings $N=4,6,8,10$.

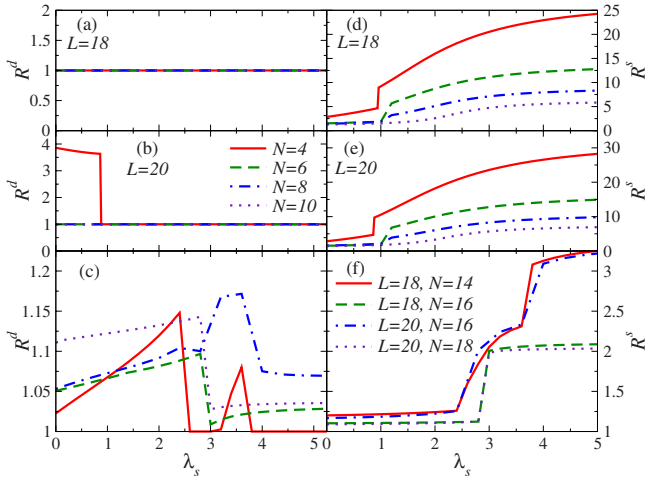

FIG. 9. (Color online) Ratio between the two lowest natural orbitals, of the d-wave (left panels) and extended-s-wave (right panels) density matrices, as a function of λ_s. [(a) and (d)] Cluster with 18 sites and fillings $N=4,6,8,10$. [(b) and (e)] Cluster with 20 sites and fillings $N=4,6,8,10$. Notice that the parameter sets for (a)–(e) are all the same and given in (d). [(c) and (f)] Clusters with 18 and 20 sites and two and four holes. The parameter sets in (c) and (f) are also the same.

d-wave superconducting state generated in a lightly doped Mott insulator. The d-wave condensate occupation is low if one compares it with the one generated, for low electron filling [Figs. 7(a) and 7(b)], under the influence of a suitable value of λ_d. This low condensate occupation is a direct consequence of the strong correlations present in the system and is similar to the behavior of the condensate occupation in liquid helium, which is known to be strongly depleted due to the effects of strong interactions.

B. s-wave term

In order to further study the suggestions in Sec. IV A, we have also studied the effect of adding an extended-s-wave-superconductivity inducing term [Eq. (4)] to the plain t-J model. In Fig. 8, we explore the behavior of the fidelity metric for such a model.

Figure 8 shows that in this case small values of the control parameter $\lambda_s \leq 1$ induce almost no response in the fidelity metric at any filling. Instead, one needs a sizable magnitude of λ_s, at both low electron filling and low hole doping, to trigger a large response in g, which would signal a phase transition to an extended-s-wave superconducting state. The calculated ratio between the two lowest natural orbitals, depicted in Fig. 9, is also consistent with this observation. Only large values of λ_s enhance the extended-s-wave condensate occupation for all fillings [Figs. 9(d)–9(f)], particularly for low hole doping [Fig. 9(f)]. Interestingly, in analogy to the d-wave case for R^d, the enhancement of the ratio R^s is almost an order of magnitude larger at low electron fillings than at low hole doping, evidencing the strong depletion of the condensate that occurs in the latter case due to the presence of strong correlations.

Overall, these findings are consistent with previous exact diagonalization studies of the t-J model[45–47] that have provided numerical evidence for dominant d-wave pairing at low hole doping, absent in the opposite limit of low electron filling. Our results also show that strong correlations become more important as one approaches half-filling, where no matter which superconductivity enhancing term one introduces, the resulting condensate occupation is always small.

V. QUENCHED DISORDER

In this section, we address the question of the effect of disorder in the models and quantities studied in the previous sections for the clean case.

For the plain t-J model, in Sec. III, we have seen that the lowest natural orbital and the ratio between the lowest and second lowest natural orbitals are in general small. For that model, we focus here on the response of the fidelity metric to adding disorder to the system. Results for this quantity, averaged over different disorder realizations, are presented in Fig. 10. For weak interactions, one would expect small values of Γ to produce localization and dramatically change the nature of the ground state in the clean case. In contrast, for strong correlations, this figure illustrates that, except for the very low electron-filling case of four particles, one needs a very large disorder strength ($\Gamma > 1$) in order to trigger a large response in g. Different disorder realizations produce a large response in g for different values of Γ, hence, the various peaks that can be seen in many of the plots (notice that the results for g are presented in a semilog scale). However, the common feature for all fillings (with the exception of $N=4$) is that large responses only occur when $\Gamma > 1$. This indicates

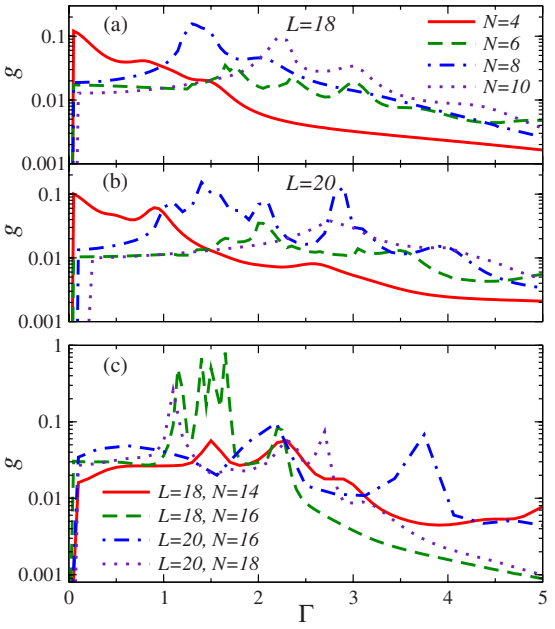

FIG. 10. (Color online) Fidelity metric of the t-J model ($J=0.3$) as a function of the disorder strength Γ. (a) Cluster with 18 sites and fillings $N=4,6,8,10$. (b) Cluster with 20 sites and fillings $N=4,6,8,10$ [the same parameter sets as in (a)]. (c) Clusters with 18 and 20 sites and two and four holes. In all cases the fidelity metric was computed averaging over 20 different disorder realizations, except for the cluster with $L=20$ and fillings $N=10$ and $N=16$ where the average was performed over ten disorder realizations.

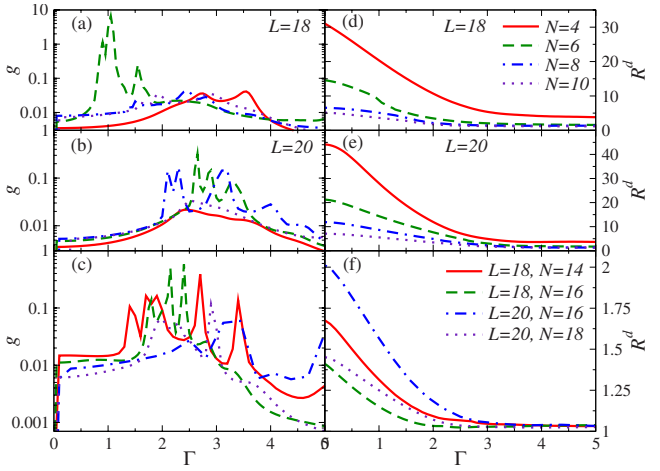

FIG. 11. (Color online) Fidelity metric (left column) and ratio between the two largest eigenvalues of the d-wave density matrix (right column) for the t-J model ($J=0.3$) with the addition of a d-wave superconductivity inducing term ($\lambda_d=1.25$) as a function of the disorder strength Γ. [(a) and (d)] Cluster with 18 sites and fillings $N=4,6,8,10$. [(b) and (e)] Cluster with 20 sites and fillings $N=4,6,8,10$ [the same parameter sets as in (a),(d)]. [(c) and (f)] Clusters with 18 and 20 sites and two and four holes. In all cases g and R^d ware computed averaging over 20 different disorder realizations, except for the cluster with $L=20$ and fillings $N=10$ and $N=16$ where the average was performed over ten disorder realizations.

that the nature of the ground state of the system in these cases is robust against nonmagnetic disorder and exemplifies the importance of strong correlations in the system. The exception is the case of very low fillings [e.g., $N=4$ for $L=18$ and $L=20$ in Fig. 10(a) and 10(b), respectively] in the t-J model, where the Gutzwiller projection plays a subdominant role.

In the clean case, the addition of a d-wave superconductivity inducing term was used to precipitate d-wave superconductivity in the t-J model and was shown to produce a large enhancement of the ratio R^d for low electron fillings and a smaller enhancement for low hole doping. Here, we study the effect of disorder in both the fidelity metric g and the ratio R^d when $J=0.3$ and $\lambda_d=1.25$.

In Fig. 11, we have plotted the evolution of g (left panel) and R^d (right panel) with increasing disorder. The results depicted in this figure were obtained averaging over the same number of disorder realizations as in Fig. 10. By comparing g in Figs. 10 and 11, one can see that the effect of adding a finite value of $\lambda_d=1.25$ is more pronounced at low fillings, where large responses in g move toward larger values of Γ ($\Gamma>2$, with the exception of $N=6$ in the $L=18$ cluster that still has a peak around $\Gamma=1$). These large responses are expected to indicate of the destruction of the superconducting ground state generated in the clean case. This can be better seen in Figs. 11(d) and 11(e), where the value of R^d is much smaller than the one in the clean case whenever a large response is seen in g [Figs. 11(a) and 11(b)].

Interestingly, in the low hole-doping regime, the behavior of the fidelity metric as a function of disorder is very similar when $\lambda_d=1.25$ and in the clean case, an indication that in this regime the ground state of the t-J model is not dramatically affected by the presence of λ_d. This marked contrast with the low electron filling is further supported if one realizes that the relative reduction of R^d is much more drastic at low electron filling than in the low hole-doping regime. Further studies using alternative numerical approaches may be needed in to clarify the scaling of these effects with system size.

Overall, our finding in the presence or absence of the superconductivity inducing term is that strong correlations generate a ground state in the t-J model that is robust against disorder.

VI. SUMMARY

Within the t-J model, we have calculated the ground-state fidelity, the d-wave and extended-s-wave condensate occupations, with and without the addition of a superconductivity inducing term, and in the clean and disordered cases.

In the clean case we find that:

(i) the plain t-J model exhibits a distinctive signature in the fidelity metric at low hole doping and small values of J that may be an indication that a continuous phase transition occurs in this regime. By studying the d-wave and extended-s-wave condensate occupations, we find that the former is favored. As expected, spin-spin (antiferromagnetic) correlations are enhanced by J in the low hole-doping regime, but they are drastically reduced by doping. Density-density correlations, on the other hand, do not exhibit any

clear signature of order as J is increased. Adding a $t'<0$ term only moves the response of the fidelity metric toward larger values of J. This is indicative of a continuous phase transition for a value of J that is larger than for the plain t-J model.

(ii) In order to better understand the nature of the phases in the plain t-J model, we added infinite range d-wave and extended-s-wave superconductivity inducing terms. For a finite value of $J=0.3$, we find that at low-hole doping arbitrarily small d-wave driving terms induce a large response in the fidelity metric, which is consistent with the plain t-J model having a d-wave superconducting ground state. In contrast, almost no response was found for low electron filling, and for the extended-s-wave superconductivity driving term for all fillings. In these latter cases one needs a large value of the driving term in order to obtain a sizable response. Interestingly, at low hole doping, we always find the condensate occupations to be small, i.e., there is a strong depletion of the (relevant) condensate no matter the symmetry of the driving term. This is an indication that, for the plain t-J model, mean-field theories based on the d-wave order parameter may not be justified.

In the dirty case, we have shown that very strong disorder is required to produce large changes in the ground state of the plain t-J model whenever the electron filling is not very low, i.e., whenever the system is strongly correlated. Adding a d-wave superconductivity inducing term was shown to leave the results for the low hole-doping regime almost unchanged with respect to the ones of the plain t-J model, while the results for the low electron-filling regime were modified to a larger extent. This is, once again, consistent with the hypothesis that the plain t-J model has a d-wave superconducting ground state for low hole doping. Future studies on the scaling of the effects and observables discussed here, with system size, could shed further light on the nature of the ground state of the t-J model and its relation to high-temperature superconductivity.

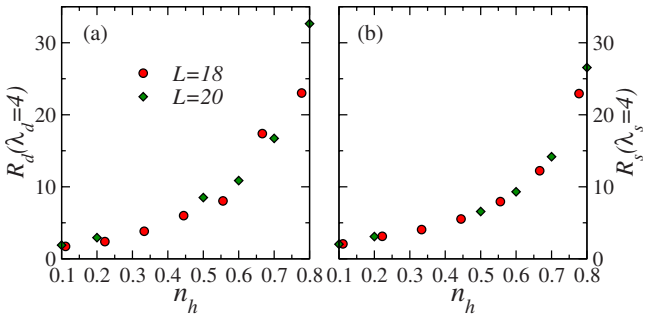

FIG. 12. (Color online) Ratio between the two lowest natural orbitals, of the d-wave (a) and extended-s-wave (b) density matrices, as a function of hole doping (n_h) for a large superconductivity inducing term with the same symmetry of the order parameter plotted. Results are presented for clusters with 18 and 20 sites. For low hole doping one can see a nearly linear dependence of the ratios R^d and R^s with n_h.

Note added in proof. With regard to the ratios (condensate occupations) R^d and R^s in the low hole doping regime, we would like to emphasize that in addition to being small (even in the presence of large superconductivity enhancing terms in the Hamiltonian) they increase linearly with increasing doping. This is shown in Fig. 12.

ACKNOWLEDGMENTS

We acknowledge support from a Startup Fund (M.R. at Georgetown University), DOE-BES Grant No. DE-FG02-06ER46319 (B.S.S. at UCSC), and NSF Grant No. DMR-0804914 (S.H. at USC). We thank G. H. Gweon, A. Muramatsu, M. Randeria, J. A. Riera, and R. T. Scalettar for helpful discussions. Computational facilities were provided by the High Performance Computing and Communications Center at the University of Southern California. M.R. is grateful to the Aspen Center for Physics where this work was finalized.

[1] J. G. Bednorz and K. A. Müller, Z. Phys. B: Condens. Matter **64**, 189 (1986).
[2] Y. Kamihara, H. Hiramatsu, M. Hirano, R. Kawamura, H. Yanagi, T. Kamiya, and H. Hosono, J. Am. Chem. Soc. **128**, 10012 (2006).
[3] E. Dagotto, Rev. Mod. Phys. **66**, 763 (1994).
[4] M. Imada, A. Fujimori, and Y. Tokura, Rev. Mod. Phys. **70**, 1039 (1998).
[5] P. A. Lee, N. Nagaosa, and X.-G. Wen, Rev. Mod. Phys. **78**, 17 (2006).
[6] M. R. Norman and C. Pepin, Rep. Prog. Phys. **66**, 1547 (2003).
[7] P. W. Anderson, P. A. Lee, M. Randeria, T. M. Rice, N. Trivedi, and F. C. Zhang, J. Phys.: Condens. Matter **16**, R755 (2004).
[8] D. J. Scalapino, Nat. Phys. **2**, 593 (2006).
[9] P. W. Anderson, Science **316**, 1705 (2007).
[10] Øystein Fischer, M. Kugler, I. Maggio-Aprile, and C. Berthod, Rev. Mod. Phys. **79**, 353 (2007).
[11] K. K. Gomes, A. N. Pasupathy, A. Pushp, S. Ono, Y. Ando, and A. Yazdani, Nature (London) **447**, 569 (2007).
[12] F. C. Niestemski, S. Kunwar, S. Zhou, S. Li, H. Ding, Z. Wang, P. Dai, and V. Madhaven, Nature (London) **450**, 1058 (2007).
[13] A. N. Pasupathy, A. Pushp, K. K. Gomes, C. V. Parker, J. Wen, Z. Xu, G. Gu, S. Ono, Y. Ando, and A. Yazdani, Science **320**, 196 (2008).
[14] J.-H. Ma, Z.-H. Pan, F. C. Niestemski, M. Neupane, Y.-M. Xu, P. Richard, K. Nakayama, T. Sato, T. Takahashi, H.-Q. Luo, L. Fang, H.-H. Wen, Z. Wang, H. Ding, and V. Madhavan, Phys. Rev. Lett. **101**, 207002 (2008).
[15] Y. Kohsaka, C. Taylor, P. Wahl, A. Schmidt, J. Lee, K. Fujita, J. W. Alldredge, J. Lee, K. McElroy, H. Eisaki, S. Uchida, D.-H. Lee, and J. C. Davis, Nature (London) **454**, 1072 (2008).
[16] J. A. Slezak, J. Lee, M. Wang, K. McElroy, K. Fujita, B. M. Andersen, P. J. Hirschfeld, H. Eisaki, S. Uchida, and J. C. Davis, Proc. Natl. Acad. Sci. U.S.A. **105**, 3203 (2008).
[17] P. A. Lee, Phys. Rev. Lett. **71**, 1887 (1993).
[18] Y. Sun and K. Maki, Phys. Rev. B **51**, 6059 (1995).

[19] A. V. Balatsky, M. I. Salkola, and A. Rosengren, Phys. Rev. B **51**, 15547 (1995).
[20] P. W. Anderson, J. Phys. Chem. Solids **11**, 26 (1959).
[21] A. Garg, N. Trivedi, and M. Randeria, Nat. Phys. **4**, 762 (2008).
[22] B. M. Andersen and P. J. Hirschfeld, Phys. Rev. Lett. **100**, 257003 (2008).
[23] M. Rigol, B. S. Shastry, and S. Haas, Phys. Rev. B **79**, 052502 (2009).
[24] F. C. Zhang and T. M. Rice, Phys. Rev. B **37**, 3759 (1988).
[25] B. S. Shastry, Phys. Rev. Lett. **63**, 1288 (1989).
[26] P. Zanardi and N. Paunkovic, Phys. Rev. E **74**, 031123 (2006).
[27] M. Cozzini, P. Giorda, and P. Zanardi, Phys. Rev. B **75**, 014439 (2007).
[28] W. L. You, Y. W. Li, and S. J. Gu, Phys. Rev. E **76**, 022101 (2007).
[29] P. Buonsante and A. Vezzani, Phys. Rev. Lett. **98**, 110601 (2007).
[30] S. Chen, L. Wang, S. J. Gu, and Y. Wang, Phys. Rev. E **76**, 061108 (2007).
[31] L. Campos Venuti and P. Zanardi, Phys. Rev. Lett. **99**, 095701 (2007).
[32] L. Campos Venuti, M. Cozzini, P. Buonsante, F. Massel, N. Bray-Ali, and P. Zanardi, Phys. Rev. B **78**, 115410 (2008).
[33] S. Garnerone, N. T. Jacobson, S. Haas, and P. Zanardi, Phys. Rev. Lett. **102**, 057205 (2009).
[34] S.-J. Gu and H.-Q. Lin, EPL **87**, 10003 (2009).
[35] R. J. Gooding, K. J. E. Vos, and P. W. Leung, Phys. Rev. B **50**, 12866 (1994).
[36] A. Nazarenko, K. J. E. Vos, S. Haas, E. Dagotto, and R. J. Gooding, Phys. Rev. B **51**, 8676 (1995).
[37] R. S. Markiewicz, S. Sahrakorpi, M. Lindroos, H. Lin, and A. Bansil, Phys. Rev. B **72**, 054519 (2005).
[38] V. I. Belinicher, A. L. Chernyshev, and V. A. Shubin, Phys. Rev. B **54**, 14914 (1996).
[39] F. Lema and A. A. Aligia, Phys. Rev. B **55**, 14092 (1997).
[40] C. Kim, P. J. White, Z. X. Shen, T. Tohyama, Y. Shibata, S. Maekawa, B. O. Wells, Y. J. Kim, R. J. Birgeneau, and M. A. Kastner, Phys. Rev. Lett. **80**, 4245 (1998).
[41] G. B. Martins, J. C. Xavier, L. Arrachea, and E. Dagotto, Phys. Rev. B **64**, 180513(R) (2001).
[42] G. Baskaran, Z. Zhou, and P. W. Anderson, Solid State Commun. **63**, 973 (1987).
[43] G. Kotliar and J. Liu, Phys. Rev. B **38**, 5142 (1988).
[44] X. G. Wen and P. A. Lee, Phys. Rev. Lett. **76**, 503 (1996).
[45] E. Dagotto, A. Moreo, R. L. Sugar, and D. Toussaint, Phys. Rev. B **41**, 811 (1990).
[46] E. Dagotto and J. Riera, Phys. Rev. B **46**, 12084 (1992).
[47] E. Dagotto and J. Riera, Phys. Rev. Lett. **70**, 682 (1993).
[48] C. S. Hellberg and E. Manousakis, Phys. Rev. B **52**, 4639 (1995).
[49] C. S. Hellberg and E. Manousakis, Phys. Rev. Lett. **78**, 4609 (1997).
[50] V. J. Emery, S. A. Kivelson, and H. Q. Lin, Phys. Rev. Lett. **64**, 475 (1990).
[51] M. Calandra, F. Becca, and S. Sorella, Phys. Rev. Lett. **81**, 5185 (1998).
[52] M. Lugas, L. Spanu, F. Becca, and S. Sorella, Phys. Rev. B **74**, 165122 (2006).
[53] J. Bardeen, L. Cooper, and J. R. Schrieffer, Phys. Rev. **108**, 1175 (1957).
[54] O. Penrose and L. Onsager, Phys. Rev. **104**, 576 (1956).
[55] P.-O. Löwdin, Phys. Rev. **97**, 1474 (1955).
[56] C. N. Yang, Rev. Mod. Phys. **34**, 694 (1962).
[57] A. J. Leggett, Rev. Mod. Phys. **73**, 307 (2001).
[58] T. Tohyama and S. Maekawa, Phys. Rev. B **49**, 3596 (1994).
[59] T. Tohyama, Phys. Rev. B **70**, 174517 (2004).
[60] L. Spanu, M. Lugas, F. Becca, and S. Sorella, Phys. Rev. B **77**, 024510 (2008).
[61] E. Khatami, A. Macridin, and M. Jarrell, Phys. Rev. B **78**, 060502(R) (2008).
[62] We should keep in mind that for finite size systems true long ranged order is impossible. In fact, the superconducting BCS type state projected to a fixed number would have a nonvanishing overlap with the normal state, especially for small system sizes.
[63] W. O. Putikka and M. U. Luchini, Phys. Rev. Lett. **96**, 247001 (2006).